Macromolecular Rapid Communications

Macromolecular Rapid Communications
www.mrc-journal.de

RESEARCH ARTICLE

Detection of Placental Extracellular Vesicle Biomarker with Terbium Coordination Polymer

Cong Minh Nguyen[1,2] | Mohamed Sallam[1,2,3] | Minh-Anh Huynh[2,4] | Yezhou Yu[1,3] | Nam-Trung Nguyen[2] | Hang Thu Ta[1,2]

[1]School of Environment and Science, Griffith University, Nathan, Australia | [2]Queensland Quantum and Advanced Technologies Research Institute, Griffith University, Nathan, Australia | [3]Griffith Institute for Drug Discovery, Griffith University, Nathan, Australia | [4]School of Engineering and Built Environment, Griffith University, Nathan, Australia

Correspondence: Nam-Trung Nguyen (nam-trung.nguyen@griffith.edu.au) | Hang Thu Ta (h.ta@griffith.edu.au)

Received: 25 September 2025 | **Revised:** 9 November 2025 | **Accepted:** 26 November 2025

Keywords: biomarker | coordination polymer | extracellular vesicles | kisspeptin-1 | mRNA | placental alkaline phosphatase | pre-eclampsia

ABSTRACT

Preeclampsia is a leading cause of maternal and fetal morbidity, with altered placental function being a key contributor to its pathogenesis. Extracellular vesicles (EVs) derived from the placenta have emerged as promising biomarkers for early diagnosis of preeclampsia. However, current EV isolation techniques face challenges related to specificity, yield, and preservation of vesicle integrity. In this proof-of-concept study, we develop a work scheme for the selective isolation of placental EVs and the detection of messenger RNA (mRNA) biomarkers. The coordination polymer is formed using terbium ions and guanosine monophosphate, with the incorporation of monoclonal antibodies targeting placental alkaline phosphatase (PLAP), a marker of trophoblast-derived EVs. Our results show that antibody-functionalized terbium coordination polymer particles efficiently captured PLAP-positive EVs, which could be gently released, preserving their integrity for downstream analysis. Transmission electron microscopy confirms the recovery of intact EVs, while Quantitative Reverse Transcription Polymerase Chain Reaction analysis is performed for the detection of KISS1 mRNA, a potential biomarker for preeclampsia. This method offers a gentle, efficient, and specific approach for EV isolation, providing a valuable tool for studying placental dysfunction and advancing biomarker analysis in preeclampsia.

1 | Introduction

Preeclampsia is a serious pregnancy-related disorder characterized by high blood pressure and damage to other organ systems, most often the liver and kidneys [1]. It usually begins after 20 weeks of pregnancy and can lead to severe complications for both the mother and the baby if left untreated [2]. Globally, preeclampsia affects 2–8% of pregnancies, making it a leading cause of maternal and fetal morbidity and mortality [3]. Risk factors for preeclampsia include first pregnancies, multifetal gestations, maternal age, and certain pre-existing medical conditions such as obesity, chronic hypertension, autoimmune, diabetes and kidney diseases [4–6]. Despite extensive research, the precise mechanisms underlying preeclampsia are still not fully understood, and effective early diagnostic markers are lacking [7, 8]. Recent studies suggest that placental dysfunction plays a central role in the pathogenesis of preeclampsia, with evidence pointing to abnormal release of factors such as soluble fms-like tyrosine kinase-1, soluble endoglin, placental growth factor, placental protein 13, and pregnancy-associated plasma protein A [2, 9]. Given the critical need for early detection and management of preeclampsia, there is a growing interest in identifying reliable biomarkers for this complication.

Extracellular vesicles (EVs) are membrane-bound particles released by cells that play crucial roles in numerous physiological

and pathological processes, intercellular communications, and have potential as biomarkers for various diseases [10]. In particular, small EVs, which carry molecular signatures reflective of their cells of origin, have emerged as promising candidates for non-invasive biomarkers. The ability to isolate and analyze EVs from maternal blood could provide valuable insights into the pathophysiology of preeclampsia and aid in its early diagnosis and monitoring. Current EV isolation methods, such as ultracentrifugation, size-exclusion chromatography, polyethylene glycol precipitation, commercial reagent kits, tangential flow filtration, present significant limitations, including low yield, contamination, scalability, time cost, and/or requiring specialized equipments [10, 11]. Immunoaffinity techniques, while offering high specificity through antibody-based targeting, often require extreme pH or high salinity buffers for elution, which can damage sensitive EV cargos [12, 13]. This underscores the need for gentler, yet equally effective, isolation methods for effective downstream analysis.

Placental alkaline phosphatase (PLAP) is an isoenzyme of alkaline phosphatase, primarily expressed in the placenta, particularly by syncytiotrophoblasts [14]. PLAP plays a key role in several physiological processes during pregnancy, including placental development and maternal-fetal nutrient exchange [15, 16]. Structurally, PLAP is a glycoprotein anchored to the cell membrane via a glycosylphosphatidylinositol anchor, making it stable and easily detectable in maternal circulation [17]. PLAP is highly expressed throughout pregnancy and is involved in dephosphorylation reactions, which are critical for regulating molecular transport and metabolism in the placenta [15, 18]. As PLAP serves as a specific marker for placental tissue, it is particularly valuable in identifying trophoblast-derived EVs that are shed into maternal blood. By focusing on these PLAP-positive EVs, researchers can gain insights into placental pathophysiology and identify early signs of complications like preeclampsia [10, 19, 20].

Kisspeptins proteins, encoded by the KISS1 gene, are primarily produced by hypothalamic nuclei and are also expressed by placental syncytiotrophoblast in developing pregnancies [21]. They are involved in the processes of trophoblast invasion and placentation, which are critical for a successful pregnancy [21]. Studies have shown that increased expression levels of KISS1 and its receptor (KISS1R) are associated with preeclampsia, indicating their role in the altered placentation process [22, 23]. It has been demonstrated that KISS1 mRNA is not only expressed in the placenta tissue but also present in extracellular vesicles (EVs) released into the cord blood of preeclampsia patients [24]. Analysis of KISS1 mRNA in circulating EVs could, therefore, could serve as a non-invasive approach to monitor placental health and predict the development of preeclampsia, potentially allowing for earlier intervention and management.

In recent years, metal coordination polymers (CPs) have attracted increasing interest in the field of bio-separation due to their tunable properties and ability to form stable complexes with biomolecules [25, 26]. Among them, lanthanide coordination polymers, particularly those using terbium ions, are notable for their strong interactions with phosphate groups, which are abundant in nucleotides and other biologically relevant molecules [27, 28]. Guanosine monophosphate (GMP), in particular, has been shown to coordinate effectively with lanthanides, making it an ideal candidate for the formation of terbium coordination polymers (TbCPs) [29, 30]. Recently, the integration of biomolecules such as antibodies into CPs has opened new avenues for biomedical applications, including targeted drug delivery, biosensing, and diagnostic imaging. Monoclonal antibodies, with their high specificity and affinity for target antigens, can be incorporated into CPs to enhance their functionality and enable targeted interactions with biological systems [31, 32].

Given the association of KISS1 mRNA with trophoblast behavior and its measurable presence in placental EVs, it is a promising target for molecular analyses in preeclampsia research. Here, we report the formation of TbCP particles with guanosine monophosphate, the incorporation of anti-PLAP antibodies, and the successful isolation and recovery of PLAP-positive EVs for KISS1 mRNA analysis. This platform was designed to allow for the gentle release of captured EVs by exploiting the competitive binding of phosphate groups to disrupt the TbCP structure, offering a novel alternative to traditional immunoaffinity methods. The proposed work scheme for our immunoaffinity capture of placental EVs using anti-PLAP@TbCP particles, followed by mRNA preeclampsia biomarker detection, is presented in Figure 1. Our approach not only facilitates the selective isolation of placental EVs but also preserves the integrity of their RNA cargo, making it a valuable tool for studying molecular markers such as KISS1 mRNA in the context of preeclampsia.

2 | Results and Discussion

First, we investigated the spontaneous formation of a terbium coordination polymer (TbCP) with guanosine monophosphate (GMP) (Figure 2A). After the addition of $TbCl_3$ into the GMP solution, the colorless precipitate was collected via centrifugation, while the supernatant was analyzed to quantify unreacted GMP. Stoichiometric analysis indicated an optimal Tb^{3+}:GMP ratio of 2:3 (Figure 2B). Therefore, this molar ratio of $TbCl_3$ and GMP was used in subsequent experiments. The majority of collected TbCP particles were found to be around 1–2 μm in diameter, with a polydispersity index (PDI) of 0.132 ± 0.015 (Figure 2C), with neutral surface zeta-potential (Figure 2D). The particles also demonstrated good stability, with no significant change in size after 24 h in water, HEPES buffer, or DMEM culture medium, as confirmed by Dynamic Light Scattering (DLS) analysis (Figure 2E).

Next, we investigated the inclusion of monoclonal antibody (anti-PLAP, Alexa488 fluorescent-tagged) into TbCP (Figure 3A). As shown in Figure 3B, increasing concentrations of terbium ion and GMP significantly improved antibody inclusion efficiency. This enhancement can be attributed to the availability of more coordination sites for bridging interactions between Tb^{3+} ions and GMP/antibody, which facilitates stronger binding and entrapment. Additionally, higher GMP concentrations promote the formation of denser supramolecular networks via hydrogen bonding and π–π stacking, further supporting antibody immobilization [29, 33]. Based on this preliminary data, we selected 0.5 mM $TbCl_3$ and 0.75 mM GMP as the optimal conditions for subsequent experiments. The anti-PLAP@TbCP particles retain the ability to capture its specific antigens, as we used the particles

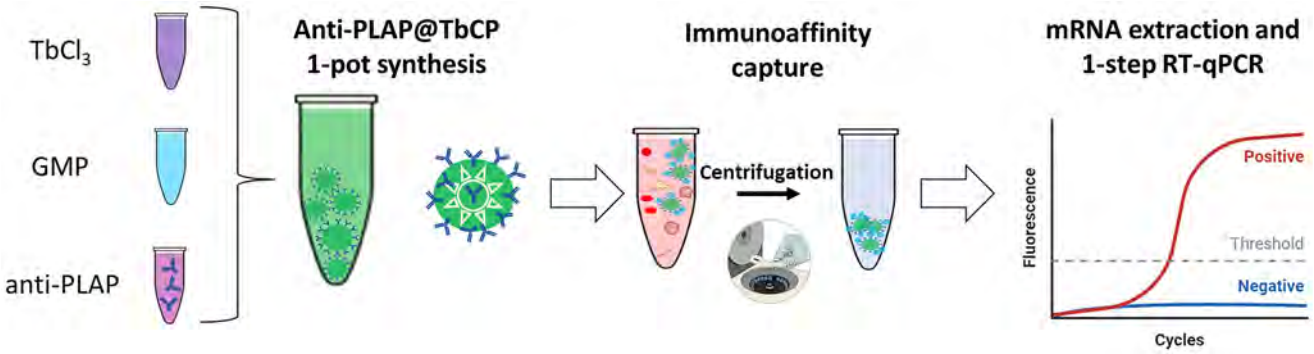

FIGURE 1 | Proposed work scheme for PLAP-positive EV isolation and mRNA biomarker detection.

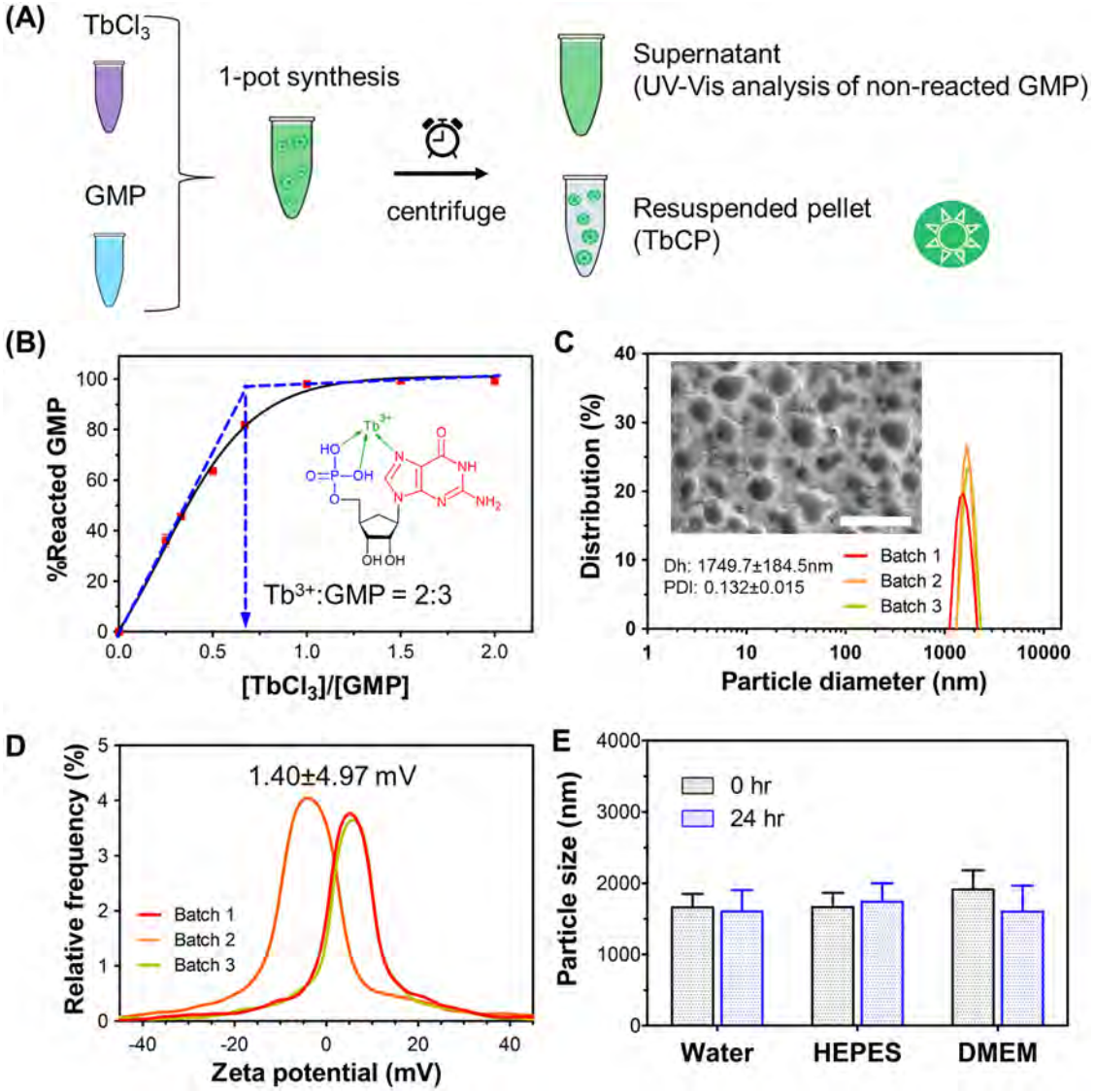

FIGURE 2 | Spontaneous formation of terbium coordination polymer (TbCP) with guanosine monophosphate (GMP). (A) Illustration of reaction and analysis; (B) Stoichiometry analysis; (C) TbCP particle size analysis with dynamic light scattering and imaging with scanning electron microscopy (inset, scale bar = 5 μm); (D) Particle zeta potential distribution; (E) Particle size before and after 24 h of incubation in water, HEPES buffer, and DMEM culture media.

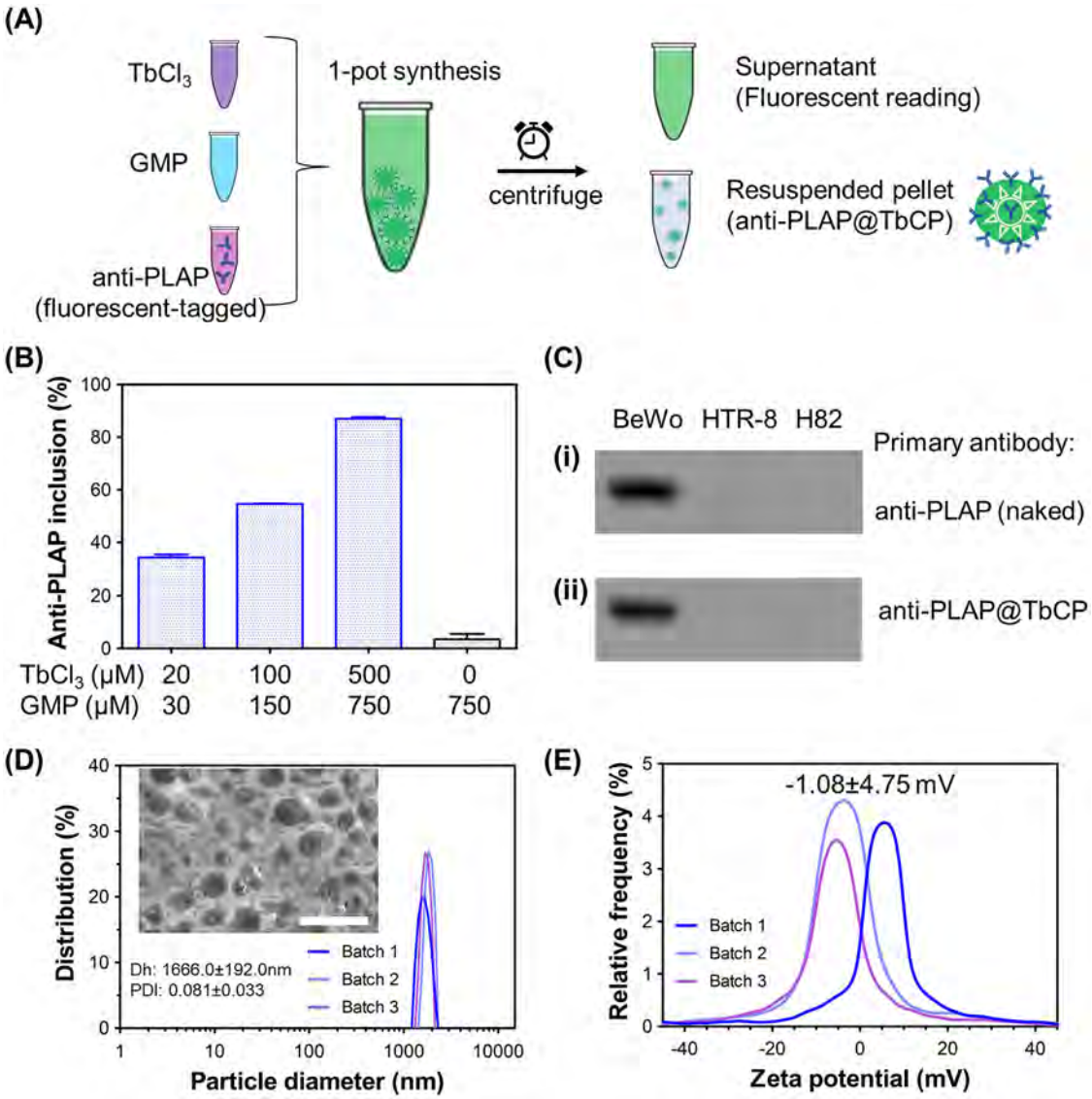

FIGURE 3 | Adaptive inclusion of monoclonal antibody (anti-PLAP) into TbCP. (A) Illustration of reaction and analysis; (B) Percentage of fluorescence-tagged anti-PLAP inclusion into TbCP at different reaction conditions; (C) Comparing naked anti-PLAP (i) and anti-PLAP@TbCP (ii) as primary antibody for western blot assay (syncytiotrophoblast BeWo cell lysates were used as a positive control, and extravillous trophoblast HTR-8 and lung cancer H82 cell lysates were used as negative controls); (D) Anti-PLAP@TbCP particle size analysis with DLS and imaging with SEM (inset scale bar = 5 μm); (E) Particle zeta potential distribution.

as primary antibodies in a Western blot assay (Figure 3C). The inclusion of antibody into TbCP did not significantly alter particle size or zeta potential (Figure 3D,E). These data strongly suggested that anti-PLAP@TbCP particles could be used for further biological applications.

We then proceeded with the isolation of placental EVs with our synthesized anti-PLAP@TbCP particles. Given that placental BeWo cell lines are well characterized for their expression of placental alkaline phosphatase (PLAP), the majority of BeWo-derived EVs were successfully captured by the anti-PLAP@TbCP particles, as anticipated (Figure 4A, blue line). In contrast, TbCP particles lacking anti-PLAP did not exhibit significant BeWo EV capture (Figure 4A, green line), confirming the specificity of the monoclonal antibody-functionalized particles.

To further assess the robustness of the platform under biologically relevant conditions, we performed a serum spike-in experiment in which BeWo EVs were resuspended in exosome-depleted serum prior to immunoaffinity isolation. In this more complex matrix, anti-PLAP@TbCP still demonstrated efficient capture of BeWo EVs (Figure 4B, blue line). The similarity in capture performance between DMEM media-resuspended samples (Figure 4A) and human serum spike-in samples (Figure 4B) underscores the high affinity of the anti-PLAP@TbCP system and its ability to isolate target EVs even in the presence of abundant serum proteins and high viscosity. This result suggests that the method can be extended to clinically relevant samples, where EV recovery is often hampered by competing biomolecules. Western blot analysis of the isolated EVs further validated their identity, demonstrating the presence of endosomal markers CD63 and

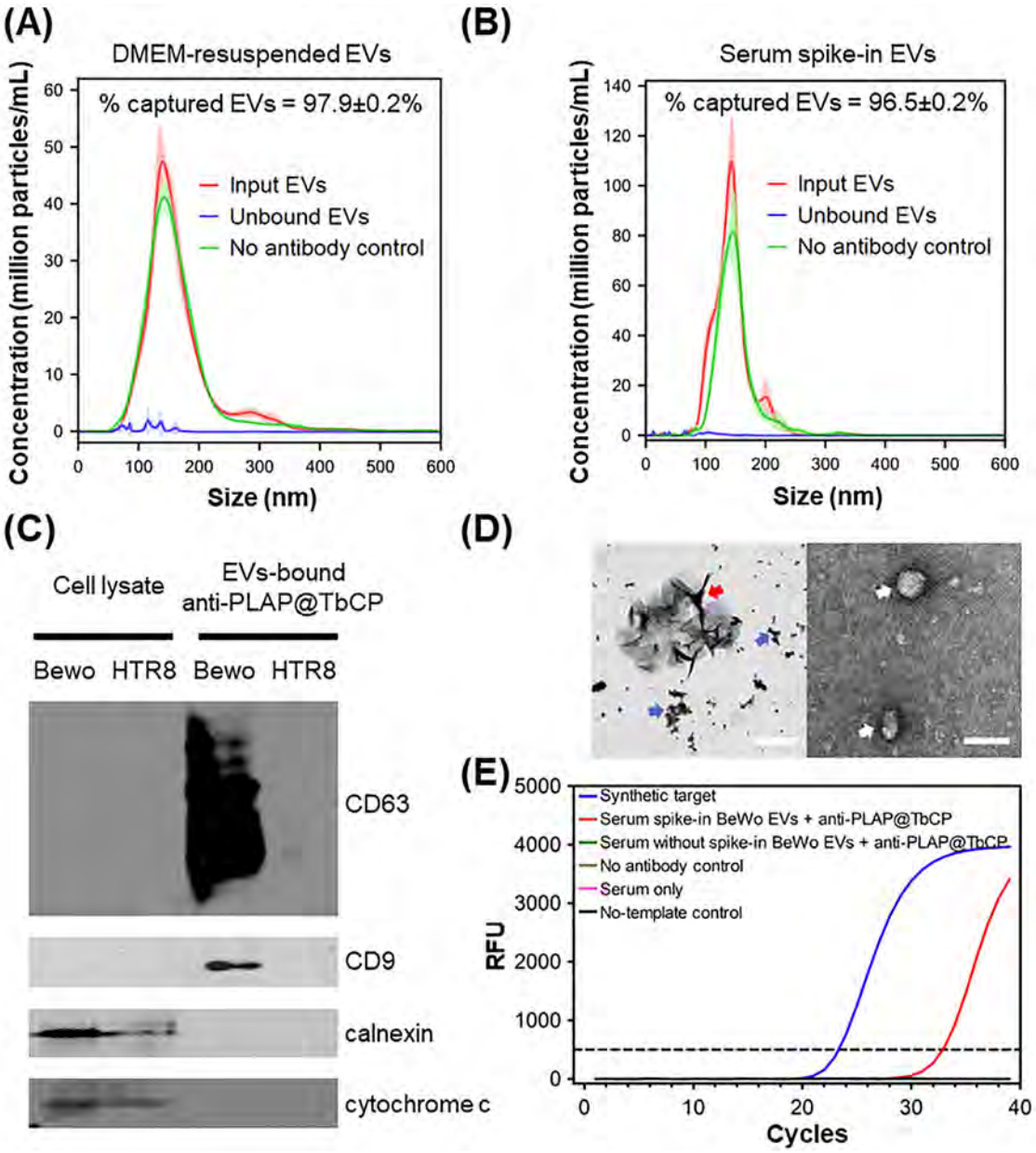

FIGURE 4 | Isolation of placental PLAP-positive EVs using anti-PLAP@TbCP. (A) Nanoparticle tracking analysis (NTA) of input and unbound EVs from DMEM media-resuspended samples; (B) NTA of input and unbound EVs from serum spike-in samples; (C) Western blot confirming the enrichment of endosomal markers (CD63 and CD9) and absence of intracellular compartment markers (calnexin and cytochrome c) in isolated placental EVs; (D) Left: TEM image of precipitated TbPO4 (red arrow) and fragments of anti-PLAP@TbCP particles (blue arrow), scale bar = 1 μm; Right: TEM image of rescued EVs, scale bar = 50 nm; (E) RT–qPCR amplification curves of KISS-1 mRNA from isolated EVs using anti-PLAP@TbCP.

CD9 while lacking the endoplasmic reticulum marker (calnexin) and the mitochondrial marker (cytochrome c) (Figure 4C).

In addition, we employed a novel strategy to recover EVs from TbCP particles. Previous studies have demonstrated that lanthanide ions, such as Tb^{3+}, exhibit strong affinity for phosphate groups due to their high oxophilicity and ability to form stable inner-sphere coordination complexes with oxygen-rich ligands [34–39]. Leveraging this property, we hypothesized that inorganic phosphate groups could effectively compete with GMP for Tb^{3+} binding, thereby disrupting the TbCP structure and facilitating the release of captured EVs. To test this hypothesis, placental EVs were first isolated using anti-PLAP@TbCP particles, after which the pellet was resuspended in a 10×phosphate buffer (100 mM, pH 7.4). After a quick centrifugation, the precipitated $TbPO_4$ and the supernatant containing released EVs were collected and analyzed with transmission electron microscopy (TEM). TEM images confirmed the structural disintegration of TbCP particles and the successful recovery of intact EVs (Figure 4D). Conventional immunoaffinity isolation techniques often rely on harsh elution conditions, such as extreme pH or high salinity, which can compromise EVs integrity. Since EVs are more stable in neutral pH solutions [40], our approach provides a milder and more EV-compatible method for efficient enrichment and processing.

Quantitative reverse transcription polymerase chain reaction (RT–qPCR) analysis of KISS1 mRNA was performed to evaluate whether the isolated EVs were suitable for downstream biomarker detection. As shown in Figure S1, RNA extracted from BeWo EVs captured with anti-PLAP@TbCP was successfully amplified, yielding amplicons with band sizes and melting peaks identical to those of the synthetic target (Figure S2). In contrast, no amplification was detected when EVs were isolated using TbCP particles lacking anti-PLAP antibodies or when anti-PLAP@TbCP was applied to isolate EVs from HTR-8 cell culture supernatant, a PLAP-negative control, validating the specificity of our systems. To further validate performance under biologically relevant conditions, ultracentrifuged BeWo EVs were spiked into serum from a healthy donor (male, 32 years old), followed by isolation with anti-PLAP@TbCP, RNA extraction, and RT–qPCR analysis. Consistent with the earlier results, only the serum sample spiked with BeWo-derived EVs produced detectable KISS1 mRNA amplification (Figure 4E), whereas the healthy serum sample containing diverse non-placental EVs showed no amplification. Collectively, these findings confirm the high specificity and efficacy of our isolation platform for capturing biomarker-rich EVs under physiologically relevant conditions.

3 | Conclusions

In this proof-of-concept study, we developed a work scheme for placental EV biomarker detection using terbium coordination polymer (TbCP). The TbCP particles, synthesized at a stoichiometric ratio of Tb^{3+}:GMP = 2:3, exhibited a consistent particle size distribution with relative stability. The inclusion of anti-PLAP monoclonal antibody into TbCP was efficient, yielding anti-PLAP@TbCP particles without altering their physicochemical properties. This system demonstrated the ability to selectively capture placental EVs and provided a gentle method for their recovery, preserving the integrity of the vesicles. The EVs isolated through this method were suitable for downstream molecular analyses, as demonstrated by RT-qPCR amplification of KISS1 mRNA, a candidate biomarker for pre-eclampsia.

To our knowledge, this is the first demonstration of a TbCP assembly with a monoclonal antibody serving as an immunoaffinity capture scaffold for placental EVs. Our simple one-pot synthesis approach achieves antibody inclusion without conventional postfunctionalization methods such as carbodiimide coupling or linker chemistry, offering the additional advantage of facile and biocompatible synthesis. The advantages of selecting TbCP as the capture platform lie in its unique coordination chemistry and structural adaptability. Terbium ions (Tb^{3+}) possess high oxophilicity and coordination numbers, forming stable yet reversible complexes with phosphate-rich ligands. This chemistry enables strong EV binding while allowing mild elution under physiological conditions, thereby preserving vesicle integrity. Conventional EV isolation techniques including ultracentrifugation, ultrafiltration, polyethylene glycol precipitation, and size-exclusion chromatography [10] are not immunocapture techniques and therefore recover all EVs from a sample. By contrast, our TbCP-based immunocapture approach was specifically designed to selectively capture PLAP-positive EVs via a monoclonal antibody. This approach offers a simple workflow that is particularly well-suited for small clinical samples, while preserving EV integrity for sensitive downstream applications. These features underscore its translational potential in prenatal diagnostics.

While the amorphous nature of the coordination polymer provides flexibility in its synthesis and applications, it also introduces potential batch-to-batch variability in particle formation and antibody integration [41, 42]. Addressing this challenge will require standardized protocols and rigorous quality control measures, focusing on precise reaction conditions, reagent quality, and antibody loading. Future work should include advanced characterization and monitoring techniques to ensure reproducibility and scalability, which are critical for clinical translation. Moreover, although the demonstrated robustness of the platform in conditioned culture media and serum-spiked samples provides a strong foundation for translational use, further validation in more complex biological matrices, such as maternal plasma or serum, will be essential to confirm its reliability and applicability in real-world clinical settings.

This study highlights the potential use of TbCP particles as a versatile tool for biomolecular isolation, offering a platform that combines specificity, efficiency, and compatibility with downstream analyses. Moreover, the system potentially allows for the incorporation of diverse antibodies, opening avenues for the application of our proposed work scheme to a broader range of applications in EV research and other bioanalytical fields.

4 | Experimental Section

4.1 | Materials

Chemicals, including terbium chloride salt and guanosine monophosphate (GMP), were procured from Merck and prepared according to specific methods. For assessment of antibody inclusion, an Alexa Fluor 488-tagged anti-placental alkaline phosphatase (anti-PLAP) antibody was used (ab270195, Abcam, UK), while for other purposes, an anti-placental alkaline phosphatase (anti-PLAP) antibody was used (ab133602, Abcam, UK). All the chemicals were used without further purification. Milli-Q water (≥18 MΩ cm) was used for reagent preparations, except in experiments involving mRNA analysis, nuclease-free water (Integrated DNA Technologies) was used instead.

4.2 | Preparation of TbCP and Anti-PLAP@TbCP

$TbCl_3$ and GMP were prepared in water and HEPES buffer (100 mM, pH 7.4), respectively. Typically, TbCP was prepared by mixing 1 mL of GMP (0.75 mM) and 1 mL of $TbCl_3$ (0.5 mM) using a magnetic stirrer at room temperature. The mixture was then incubated for 5 min with no stirring, and the precipitates were collected and washed 3 times with Milli-Q water by centrifugation at 10 000 × g for 5 min. Finally, the precipitates were redispersed in the desired volume of Milli-Q water and sonicated before performing particle analysis.

To prepare the anti-PLAP@TbCP, 1 mL of GMP (0.75 mM) was mixed with anti-PLAP (100 μg/mL, 4 μL) to obtain a homogenous solution, followed by the addition of 1 mL of $TbCl_3$ (0.5 mM) while mixing using a magnetic stirrer. The mixture was then

incubated for 5 min with no stirring, and the precipitates were collected and washed 3 times with Milli-Q water by centrifugation at 10 000×g for 5 min. The final precipitates were resuspended in ice-cold HEPES buffer and dispersed by sonication before further application.

4.3 | Stoichiometry Analysis

For stoichiometry analysis, 1 mL of GMP (0.75 mM) was mixed with different concentrations of $TbCl_3$. After centrifugation, the quantity of unreacted GMP (in supernatant fraction) was assessed by absorbance at 253 nm reading via a NanoDrop ND-1000 UV–Vis Spectrophotometer (Nanodrop Technologies, Wilmington, DE), following a GMP calibration curve (Figure S3).

4.4 | Particle Size Analysis and Zeta Potential Measurement

To determine the particle hydrodynamic size, 100 µL of particles were suspended in 900 µL of water and placed in a LiteSizer 500 (Anton Paar) for analysis using a disposable cuvette (10 × 10 × 45 mm). 1 mL of the same mixture was measured in an omega cuvette utilizing the Zeta measurement mode for the Zeta potential analysis, following Helmholtz-Smoluchowski equation.

4.5 | Particle Imaging with Scanning Electron Microscopy

Aqueous solutions of particles were dried on an aluminum foil for scanning electron microscopy (SEM) imaging. The samples were sputter-coated with gold and analyzed with a Apreo 2 SEM system (Thermo Fisher Scientific) at 10 kV, magnification 10 000x, Everhart–Thornley detector.

4.6 | Transmission Electron Microscopy

The samples were drop-mounted onto Formvar/carbon-coated 200 mesh copper grids (for 2–3 min), the excess water was removed, and the samples were negatively stained with 2% aqueous uranyl acetate for 2 min. Afterward, the excess water was removed. Once air-dried, the samples were imaged on a JEOL 1400 transmission electron microscope operated at 120 kV and mounted with a TVIPS 2K F216 CCD camera at the Central Analytical Research Facility (Queensland University of Technology).

4.7 | Monoclonal Antibody Inclusion Efficiency

After the inclusion of fluorescent antibodies into TbCP, the samples were centrifuged. The fluorescence intensity (RFU) of the supernatant indicates the quantity of non-binding antibodies. Antibody inclusion (%) was calculated with the following equation:

$$Antibody\ inclusion\ (\%) = \left(1 - \frac{Fluorescent\ of\ supernatant - Blank}{Fluorescent\ of\ naked\ antibodies - Blank}\right) \times 100\%$$

4.8 | Western Blot Analysis

For each cell line, a pellet containing 2×10^6 cells was lysed in 100 µL of sample buffer (50 mM Tris-HCl pH 6.8, 0.1 M dithiothreitol, 2% sodium dodecyl sulfate (SDS), 10% glycerol and 0.001% bromophenol blue) and denatured at 95°C for 5 min. A total of 15 µL of the lysate was resolved by 8% SDS–polyacrylamide gel electrophoresis (SDS–PAGE) and transferred to a polyvinylidene difluoride (PVDF) membrane using a Trans-Blot system (Bio-Rad, Hercules, CA, USA). The PVDF membrane was blocked with 3% bovine serum albumin (BSA) in Tris-buffered saline with 0.1% Tween-20 (TBS-T) for 1 h at room temperature, and subsequently incubated for 2 h with either an anti-placental alkaline phosphatase (PLAP) antibody (ab133602, Abcam, Cambridge, UK) (10 ng/mL, diluted in blocking buffer) or anti-PLAP@TbCP (containing an equivalent amount of anti-PLAP antibodies) as primary antibody. After washing, the membrane was incubated with an HRP-conjugated goat antirabbit secondary antibody (1706515; Bio-Rad) (1:4000; diluted in blocking buffer) for 2 h at room temperature. Chemiluminescent detection was carried out with SuperSignal West Pico Chemiluminescent Substrate (Thermo Scientific) and visualized on a Sapphire Biomolecular Imager (Azure Biosystems, Dublin, CA, USA).

To verify the presence of CD9 and CD63 and the absence of calnexin and cytochrome c in isolated EVs, a similar Western blot was performed. Enriched EVs were lysed in 5× sample buffer and heated at 95°C for 5 min. A volume of 15 µL of the lysed sample was resolved by 10% SDS–polyacrylamide gel electrophoresis (SDS–PAGE) and transferred to PVDF membranes by transblotting (Bio-Rad, Hercules, CA, USA). The PVDF membrane was blocked for 1 h at room temperature in blocking buffer and then incubated for 2 h with either anti-CD9 (10626D, Invitrogen, MA, USA), anti-CD63 HRP conjugated (NBP2-42225H, Novus Biologicals, CO, USA), anti-calnexin (GT1560, Invitrogen, MA, USA), or anti-cytochome c (7H8.2C12, Invitrogen, MA, USA) primary antibodies at a dilution of 1:1000 in blocking buffer. After washing, the membrane was incubated with corresponding HRP-conjugated secondary antibodies (1706515 and 1706516; Bio-Rad) (1:4000) for 2 h at room temperature. For anti-CD63 HRP conjugated, no secondary antibodies incubation were required. Chemiluminescent detection was carried out with SuperSignal West Pico Chemiluminescent Substrate kit (Thermo Scientific) following supplier's manual instructions. Each West blotting experiment was performed in duplicate, with representative blots are shown in figures.

4.9 | Isolation of PLAP-Positive EVs

BeWo cell line (ATCC CCL-98) was grown in F12 medium (ATCC 30-2006) supplemented with 10% fetal bovine serum (FBS, Gibco A3160902) and 1% Penicillin-Streptomycin (Gibco 15140148) until 60% confluent. Culture medium was then replaced with media containing 10% exosome-depleted FBS (Gibco A2720801) and cells were grown for another 60 h. After that, culture media from several flasks were collected and pooled together, filtered, and ultracentrifuged. A volume of 50 mL of cell culture media was 0.22 µm-filtered and ultracentrifuged at 100 000×g

for 90 min. The invisible pellet was resuspended in either 1 mL of DMEM media or 0.5 mL of exosome-depleted FBS and considered the inputs for EVs isolation. The 0.2 mL of input EVs was mixed with 0.8 mL of anti-PLAP@TbCP overnight at 4°C with rocking. After centrifugation at 10 000×g for 5 min, the supernatant containing the unbound EVs was collected for nanoparticle tracking analysis to estimate the EVs capture efficiency.

A total of 10 mL of citrated blood was collected from a healthy donor (male, 32 years old) and mixed with 250 µL of 1 M $CaCl_2$ (prepared in 0.9% NaCl) to induce coagulation at room temperature for 1 h. The sample was then centrifuged at 2000×g for 30 min at 4°C, and the supernatant was collected as healthy serum. BeWo-derived EVs pellet (prepared by ultracentrifugation as previously described) were spiked into 0.5 mL of serum to mimic disease condition and subsequently used as input for EV isolation following the same procedure.

4.10 | Nanoparticle Tracking Analysis

Nanoparticle tracking analysis (NTA) was carried out with a NanoSight NS300 system (Malvern, PA, USA). The samples were diluted with PBS (if necessary) and subsequently introduced into the instrument using the following script: PUMPLOAD, REPEATSTART, PRIME, DELAY 10, CAPTURE 30, and REPEAT 5. Videos were recorded at a camera level of 10, a camera shutter speed of 20 ms and a camera gain of 600; these settings were kept constant between samples. Each video was subsequently analyzed to determine the concentration, mean, mode, and size distribution of EVs.

4.11 | KISS1 mRNA Detection

Total mRNA was extracted from EVs via a RNeasy Mini Kit (Qiagen, Hilden, Germany) following the manufacturer's instructions. After that, a standard 1-step RT–qPCR assay was performed using a SYBR Green Quantitative RT–PCR Kit (QR0100; Sigma Chemical Co., St. Louis, Mo.) following the manufacturer's suggested protocol. Melting curve analysis was carried out from 60°C to 95°C with 0.5°C increments in a CFX96 Thermocycler (Bio-Rad, CA, USA).

The FW primer used was 5'-CAC CCT CTG GAC ATT CAC C-3', and the RV primer used was 5'-CCA AGA AAC CAG TGA GTT CAT C-3'. These primers were obtained from Integrated DNA Technologies (Iowa, USA). For positive control, synthetic KISS-1 mRNA was synthesized from gBlock gene fragments (Integrated DNA Technologies) using a HiScribe T7 Quick High Yield RNA Synthesis Kit (E2050S, NEB, MA, USA) following the manufacturer's instructions.

A 2% agarose gel was prepared in 1× TAE buffer with the addition of 10 µL of SYBR Safe (Invitrogen, MA, USA) per 100 mL of gel. A 10-µL sample was mixed with 2 µL of 6× gel loading dye (Thermo Fisher Scientific, USA), and electrophoresis was performed at 80 V for 90 min. Gel imaging was performed with a Gel Doc XR+ Imaging System (Bio-Rad).

Author Contributions

C.M.N.: Conceptualization, Methodology, Resources, Investigation, Data Curation, Formal Analysis, Validation, Visualization, Writing – Original Draft Preparation, Review & Editing; M.S.: Conceptualization, Methodology, Resources, Investigation, Validation; M.A.H.: Investigation, Methodology, Validation, Writing – Original Draft Preparation, Review & Editing; Y.Y.: Investigation, Methodology, Resources, Validation; N.T.N.: Supervision, Writing – Review & Editing; H.T.T.: Supervision, Writing – Review & Editing.

Acknowledgements

This work was supported by the Griffith University Higher Degree Research Scholarship. The authors thank Prof. Carlos Salomon (University of Queensland), Dr. Narshone Soda (Queensland Micro- and Nanotechnology Centre), and Waqar Afridi (Griffith University) for their generous contributions to the materials. The authors acknowledge the facilities and the scientific and technical assistance of the Central Analytical Research Facility, the Institute of Health and Biomedical Innovation, the Queensland University of Technology, and the Microscopy Australia Facility at the Centre for Microscopy and Microanalysis, University of Queensland.

Conflicts of Interest

The authors declare no conflicts of interest.

Data Availability Statement

All data have been included in the main manuscript and supporting information document.

References

1. "Gestational Hypertension and Preeclampsia: ACOG Practice Bulletin, Number 222," *Obstetrics & Gynecology* 135 (2020): 237–260.

2. M. Rybak-Krzyszkowska, J. Staniczek, A. Kondracka, et al., "From Biomarkers to the Molecular Mechanism of Preeclampsia-A Comprehensive Literature Review," *International Journal of Molecular Sciences* 24 (2023): 13252.

3. N. Atluri, T. K. Beyuo, S. A. Oppong, C. A. Moyer, and E. R. Lawrence, "Challenges to Diagnosing and Managing Preeclampsia in a Low-resource Setting: a Qualitative Study of Obstetric Provider Perspectives from Ghana," *PLOS Global Public Health* 3 (2023): 0001790.

4. S. Hernández-Díaz, S. Toh, and S. Cnattingius, "Risk of Pre-eclampsia in First and Subsequent Pregnancies: Prospective Cohort Study," *Bmj* 338 (2009): b2255.

5. N. S. Boghossian, E. Yeung, P. Mendola, et al., "Risk Factors Differ between Recurrent and Incident Preeclampsia: A Hospital-based Cohort Study," *Annals of Epidemiology* 24 (2014): 871–877.e3.

6. K. Duckitt and D. Harrington, "Risk Factors for Pre-eclampsia at Antenatal Booking: Systematic Review of Controlled Studies," *Bmj* 330 (2005): 565.

7. M. Liu, Y. Niu, K. Ma, et al., "Identification of Novel First-trimester Serum Biomarkers for Early Prediction of Preeclampsia," *Journal of Translational Medicine* 21 (2023): 634.

8. M. Yao, Y. Xiao, Z. Yang, et al., "Identification of Biomarkers for Preeclampsia Based on Metabolomics," *Clinical Epidemiology* 14 (2022): 337–360.

9. T. T. T. Pham, D. P. Tran, M. C. Nguyen, et al., "A Simplified Point-of-care Testing Approach for Preeclampsia Blood Biomarkers Based on Nanoscale Field Effect Transistors," *Nanoscale* 13 (2021): 12279–12287.

10. C. M. Nguyen, M. Sallam, M. S. Islam, et al., "Placental Exosomes as Biomarkers for Maternal Diseases: Current Advances in Isolation, Characterization, and Detection," *ACS Sensors* 8 (2023): 2493–2513.

11. S. Williams, A. R. Jalal, M. P. Lewis, and O. G. Davies, "A Survey to Evaluate Parameters Governing the Selection and Application of Extracellular Vesicle Isolation Methods," *Journal of Tissue Engineering* 14 (2023): 20417314231155114.

12. J. Fitzgerald, P. Leonard, E. Darcy, S. Sharma, and R. O'Kennedy, eds. D. Walls and S.T. Loughran, in *Protein Chromatography: Methods and Protocols*, (2017), 27.

13. T.-W. Lo, Z. Zhu, E. Purcell, et al., "Microfluidic Device for High-throughput Affinity-based Isolation of Extracellular Vesicles," *Lab on a Chip* 20 (2020): 1762–1770.

14. K. Leitner, R. Szlauer, I. Ellinger, A. Ellinger, K.-P. Zimmer, and R. Fuchs, "Placental Alkaline Phosphatase Expression at the Apical and Basal Plasma Membrane in Term Villous Trophoblasts," *Journal of Histochemistry & Cytochemistry* 49 (2001): 1155–1164.

15. C. Salomon, M. J. Torres, M. Kobayashi, et al., "A Gestational Profile of Placental Exosomes in Maternal Plasma and Their Effects on Endothelial Cell Migration," *PLoS ONE* 9 (2014): 98667.

16. R. Makiya and T. Stigbrand, "Placental Alkaline Phosphatase as the Placental IgG Receptor," *Clinical Chemistry* 38 (1992): 2543.

17. A. R. Borges, F. Link, M. Engstler, and N. G. Jones, "The Glycosylphosphatidylinositol Anchor: A Linchpin for Cell Surface Versatility of Trypanosomatids," *Frontiers in Cell and Developmental Biology* 9 (2021): 720536.

18. A. Parveen, S. Mishra, M. Srivastava, et al., "Circulating Placental Alkaline Phosphatase Expressing Exosomes in Maternal Blood Showed Temporal Regulation of Placental Genes," *Frontiers in Medicine* 8 (2021): 758971.

19. C. Palma, J. Jellins, A. Lai, et al., in *New Frontiers: Extracellular Vesicles*, eds. P. Mathivanan and P. Fon, (2021), 455.

20. T. Awoyemi, S. Jiang, and M. Rahbar, et al., "MicroRNA analysis of medium/large placenta extracellular vesicles in normal and preeclampsia pregnancies," *Frontiers in Cardiovascular Medicine* 11 (2024): 1371168.

21. A. Erin, P. Elaine, W. Michael, and M. Courtney, in *Infertility and Assisted Reproduction*, ed. W. Wei-Hua, (IntechOpen 2021), 12.

22. R. V. Kapustin, A. O. Drobintseva, E. N. Alekseenkova, et al., "Placental Protein Expression of Kisspeptin-1 (KISS1) and the Kisspeptin-1 Receptor (KISS1R) in Pregnancy Complicated by Diabetes Mellitus or Preeclampsia," *Archives of Gynecology and Obstetrics* 301 (2020): 437–445.

23. J. E. Cartwright and P. J. Williams, "Altered Placental Expression of Kisspeptin and Its Receptor in Pre-eclampsia," *Journal of Endocrinology* 214 (2012): 79–85.

24. L. Hu, J. Ma, M. Cao, et al., "Exosomal mRNA and lncRNA profiles in cord blood of preeclampsia patients," *The Journal of Maternal-Fetal & Neonatal Medicine* 35 (2022): 8199–8209.

25. Y. Li, H. Gao, Y. Jin, R. Zhao, and Y. Huang, "Peptide-derived Coordination Frameworks for Biomimetic and Selective Separation," *Analytical and Bioanalytical Chemistry* 415 (2023): 4079–4092.

26. E. Khare, N. Holten-Andersen, and M. J. Buehler, "Transition-metal Coordinate Bonds for Bioinspired Macromolecules with Tunable Mechanical Properties," *Nature Reviews Materials* 6 (2021): 421–436.

27. J. Gao, C. Wang, and H. Tan, "Lanthanide/Nucleotide Coordination Polymers: An Excellent Host Platform for Encapsulating Enzymes and Fluorescent Nanoparticles to Enhance Ratiometric Sensing," *Journal of Materials Chemistry B* 5 (2017): 7692–7700.

28. S. Li, S. Jansone-Popova, and D. Jiang, "Insights into Coordination and Ligand Trends of Lanthanide Complexes from the Cambridge Structural Database," *Scientific Reports* 14 (2024): 11301.

29. R.-R. Gao, S. Shi, Y.-J. Li, M. Wumaier, X.-C. Hu, and T.-M. Yao, "Coordination Polymer Nanoparticles from Nucleotide and Lanthanide Ions as a Versatile Platform for Color-tunable Luminescence and Integrating Boolean Logic Operations," *Nanoscale* 9 (2017): 9589–9597.

30. L. Chen, P. Huang, H. Tan, and L. Wang, "A Terbium(iii)-based Coordination Polymer for Time-resolved Determination of Hydrogen Sulfide in human Serum via Displacement of Copper(ii)," *Analytical Methods* 9 (2017): 1004–1010.

31. J. Qin, N. Guo, J. Yang, and Y. Chen, "Recent Advances of Metal-Polyphenol Coordination Polymers for Biomedical Applications," *Biosensors* 13 (2023): 776.

32. Y. Sun, J. Ma, F. Ahmad, et al., "Bimetallic Coordination Polymers: Synthesis and Applications in Biosensing and Biomedicine," *Biosensors* 14 (2024): 117.

33. M. Ilyas, M. A. Khan, L. Xiong, et al., "Enhancements of the First and Second Hyperpolarizability of a GMP Coordination Polymer: Crystal Structure and Computational Studies," *Dalton Transactions* 54 (2025): 5921–5934.

34. V. C. Pierre and R. K. Wilharm, "Design Principles and Applications of Selective Lanthanide-Based Receptors for Inorganic Phosphate," *Frontiers in Chemistry* 10 (2022): 821020.

35. T. L. M. Martinon and V. C. Pierre, "Luminescent Lanthanide Probes for Cations and Anions: Promises, Compromises, and Caveats," *Current Opinion in Chemical Biology* 76 (2023): 102374.

36. L. J. Martin and B. Imperiali, in *Peptide Libraries: Methods and Protocols*, ed. R. Derda, (Springer 2015), 201.

37. S. E. Bodman and S. J. Butler, "Advances in Anion Binding and Sensing Using Luminescent Lanthanide Complexes," *Chemical Science* 12 (2021): 2716–2734.

38. P. B. Guseva, A. R. Badikov, O. S. Butorlin, et al., "Complexation of Lanthanides(III) Ions with Terephthalic Acid in Aqueous Solutions by Potentiometric Titration Combined with Photoluminescence Spectroscopy," *Chemistry (Weinheim An Der Bergstrasse, Germany)* 7 (2025): 57.

39. N. Jordan, T. Thoenen, S. Starke, K. Spahiu, and V. Brendler, "A Critical Review of the Solution Chemistry, Solubility, and Thermodynamics of Europium: Recent Advances on the Eu3+ Aqua Ion and the Eu(III) Aqueous Complexes and Solid Phases with the Sulphate, Chloride, and Phosphate Inorganic Ligands," *Coordination Chemistry Reviews* 473 (2022): 214608.

40. Y. Cheng, Q. Zeng, Q. Han, and W. Xia, "Effect of pH, temperature and freezing-thawing on quantity changes and cellular uptake of exosomes," *Protein & Cell* 10 (2019): 295–299.

41. Z. Lin, J. J. Richardson, J. Zhou, and F. Caruso, "Direct Synthesis of Amorphous Coordination Polymers and Metal–organic Frameworks," *Nature Reviews Chemistry* 7 (2023): 273–286.

42. S. Abtahi, N. Hendeniya, S. T. Mahmud, G. Mogbojuri, C. L. Iheme, and B. Chang, "Metal-Coordinated Polymer–Inorganic Hybrids: Synthesis, Properties, and Application," *Polymer* 17 (2025): 136.

Supporting Information

Additional supporting information can be found online in the Supporting Information section.

Supporting File: marc70161-sup-0001-SuppMat.docx.

Supporting Information

Detection of placental extracellular vesicle biomarker with terbium coordination polymer

Cong Minh Nguyen[ab], *Mohamed Sallam*[abd], *Minh-Anh Huynh*[bc], *Yezhou Yu*[ad], *Nam-Trung Nguyen*[b]*, *Hang Thu Ta*[ab]*

[a] School of Environment and Science, Griffith University, Nathan, Australia

[b] Queensland Quantum and Advanced Technologies Research Institute, Griffith University, Nathan, Australia

[c] School of Engineering and Built Environment, Griffith University, Nathan, Australia

[d] Griffith Institute for Drug Discovery, Griffith University, Nathan, Australia

* Corresponding author: h.ta@griffith.edu.au and nam-trung.nguyen@griffith.edu.au

Supplemental data figures

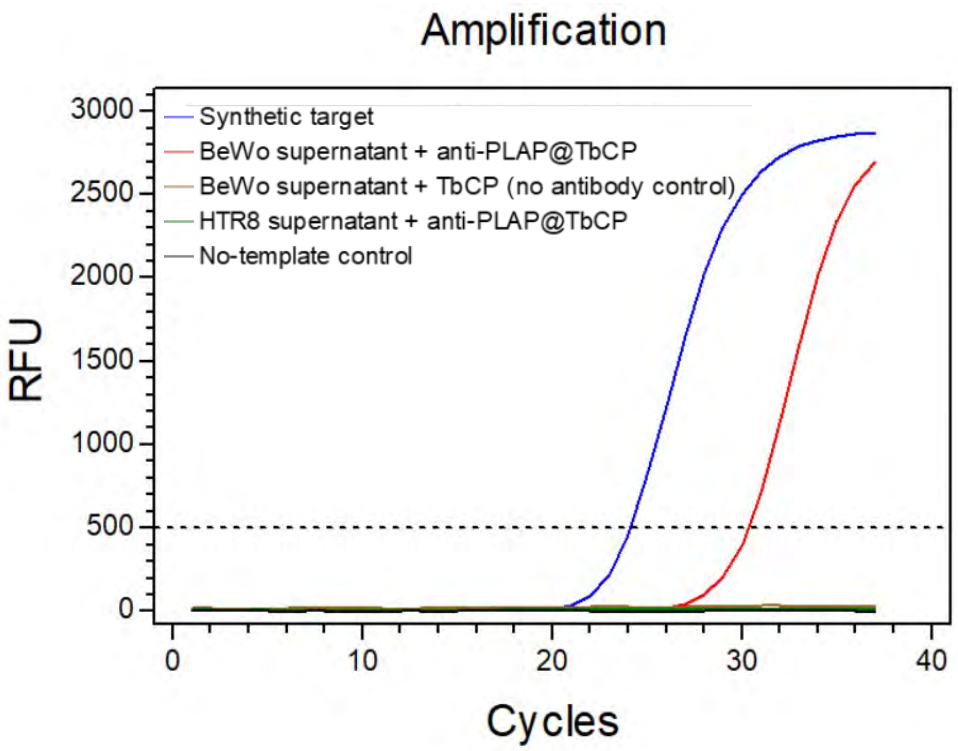

Figure S1. Quantitative reverse transcription polymerase chain reaction (RT–qPCR) analysis of KISS1 mRNA from EVs captured by TbCP in cell culture media (CCM). NTC = no-template control.

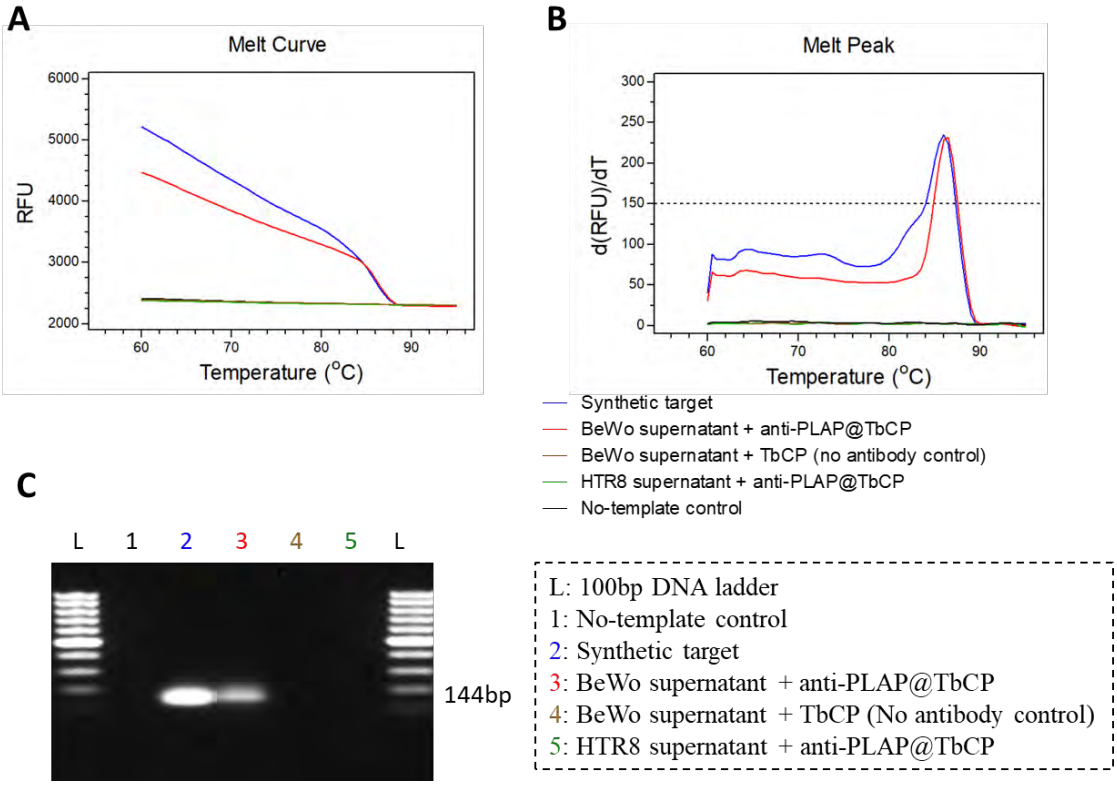

Figure S2. Analysis of amplicons with **(A)** melting curve, **(B)** melting peak, and **(C)** gel electrophoresis.

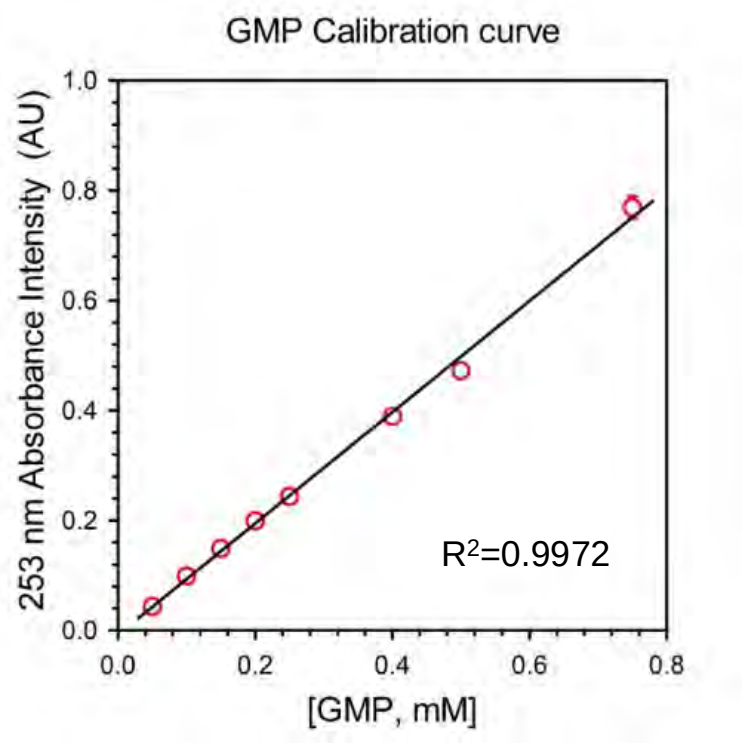

Figure S3. Guanosine monophosphate (GMP) calibration curve.